

INVESTIGATION OF GRAVITATIONAL EFFECTS IN SOLUTION GAS DRIVE VIA PORE NETWORK MODELLING: RESULTS FROM NOVEL CORE-SCALE SIMULATIONS

Bondino I. (1), Hamon G. (2), Long J. (2), McDougall S.R. (3)
(1) TOTAL UK E&P Ltd (2) TOTAL (3) Heriot-Watt University Edinburgh

This paper was prepared for presentation at the International Symposium of the Society of Core Analysts held in Calgary, Canada 10-12 September, 2007

ABSTRACT

In this work a mature pore scale network model for oil depressurisation has been used for the first time to simulate typical core scales, initiating a new phase in the use of such techniques for core analysis. Important results clearly demonstrate the fact that it is now possible to reproduce the physical scale and pressure dependent balance of forces acting along the entire height of a vertically-mounted laboratory core during a solution gas drive experiment — without the need for upscaling pore-to-core methodologies. Now it has become possible to reproduce the complexity of an evolving gravity/capillarity force balance and investigate its nonlinear impact upon bubble break-up and coalescence phenomena throughout the course of an experiment. Using the macroscale approach explained above, we investigate the effect of varying the underlying Bond number of a simulation and examine sensitivities to the rate of depletion (bubble densities), the fluid properties, system scale, and the petrophysical characteristics of the sample. We show that relative permeabilities can be predicted according to the particular flow regimes exhibited by gas (dispersed and/or continuous) and demonstrate how flow is largely determined by the size and density of gas clusters, whether originating from nucleation or from break-up of larger structures during migration. In conclusion we show the different ways in which gas saturation gradients can develop along the height of a core sample. The results are compared against available experimental data — specifically, in situ gas saturation profiles and production histories — from equivalent sized samples (10 centimetres in height). These comparisons are utilised to provide a physical description of the mechanisms taking place during the experiments.

INTRODUCTION

Solution gas drive is the process by which bubbles nucleating in a porous medium undergoing depressurization contribute, as they grow, to the expulsion of oil out of the pore space. This is a natural recovery mechanism which has been considered for implementation in a number of fields in the North Sea and elsewhere (Ligthelm et al, 1997; Beecroft et al, 1999; Drummond et al, 2001; Petersen et al, 2004; Ayyalasomayajula et al, 2006) both in primary and tertiary mode. Unfortunately the features of the physical process appear sometimes elusive. It has long been known (Kennedy and Olson, 1952) that recoveries increase with depletion rate as more bubbles nucleate, but more precise or quantitative predictions are difficult to make. As an

example, Egermann and Vizika (2000), Goodfield and Goodyear (2003) and Ayyalasomayajula et al (2006) have shown that relative permeabilities obtained by history matching experiments with reservoir simulators often show non conventional behavior; the history match requires gas curves that remain extremely low even at high gas saturations. Bauget et al (2003) pointed to the fact that conventional reservoir simulators are of little help in providing representative flow parameters to reservoir engineers as they do not incorporate the complex physics of the process, which includes non equilibrium behavior (supersaturation), non Darcian flow of disconnected bubbles, and the pressure dependency of a range of parameters (interfacial tension, bubble density, *inter alia*). They observed that a comprehensive tool that could be very useful for the determination of relative permeabilities and critical gas saturation could be represented by pore scale networks models: these tools can incorporate the most relevant physics into a geometrical and topologically equivalent representation of the porous rock. However, they noted that pore scale models could simulate only microscale scenarios with a limited numbers of pores, and therefore concluded that they would be of little use in practical applications. This is generally true in light of the fact that microscale setups can generally account for capillary-controlled cases only, whereas in practical cases, such as in core experiments, gravitational and viscous effects can generally become important (Skauge et al, 1999; Piccavet et al, 2006).

In the work presented here, we propose a macroscale application of pore-scale modeling, which allows us to overcome the aforementioned difficulties. We show that, using modern computational facilities, it is now possible to simulate multi-phase flow and molecular diffusion (as required for the problem under examination) at the appropriate laboratory scale using very large pore-scale networks. We explore the *macroscopic implications* of the *pore-scale* physics and address issues such as gravitationally driven flow, the pressure evolution of the gravity/capillarity force balance (Bond number) and core-scale gas saturation profiles.

PORE SCALE MODELING OF OIL DEPLETION WITH GRAVITY Stage Of Gravitationally Biased Bubble Growth

The contributions to bubble growth come mainly from the increase in bubble pressure P_g due to molecular diffusion of dissolved gas components into the bubble and to the decrease in liquid pressure P_l . Both effects are included in the pore scale model (McDougall and Mackay, 1998). Furthermore gravitational bias emerges if the local (pore level) hydrostatic pressure term is large enough to perturb the local capillary pressure thresholds.

In a 2-phase gas-oil system (gas strongly non wetting to oil), the oil-filled pore with the minimum capillary entry threshold must be identified around all perimeter sites surrounding a gas structure:

$$P_c^{\min} = \min_i \left(\frac{2\sigma_{go}^i}{r_i} - \Delta\rho g h_i \right) \quad (1)$$

where the index i runs over all the oil-filled perimeter pores, σ_{go} is the gas-oil interfacial tension, r_i the capillary entry radius, $\Delta\rho$ the density difference between oil and gas, g the

gravitational constant and h_i the distance of the oil-filled pore from the bottom of the bubble ($0 \leq h_i \leq h_{bubble}$), which can span several pores. Once the correct pore has been identified from Eq. (1), expansion in that pore takes place only if:

$$(P_g - P_o) > P_c^{min} \quad (2)$$

where P_g and P_o are the gas and oil pressures respectively. Therefore if the interfacial tension is low and/or the gas structure tall, capillary entry thresholds can more easily be overcome towards the top of the gas structure: the bottom of the structure remains at the same datum position and the top advances upwards.

Stage Of Gravitational Bubble Migration

If the capillary entry threshold is spontaneously overcome ($P_c^{min} < 0$) the bubble can spontaneously migrate: at the pore level this translates in a gas drainage event followed by one or more oil imbibition events. The succession of these events maintains the bubble volume constant as the structure moves upwards. The implementation of bubble migration used here extends that described in McDougall and Mackay (1998).

One problem to overcome when dealing with spontaneous migration is the question of which velocity to assign to a migrating gas-oil interface (see Corapcioglu et al, 2004). In the method presented here, we make the assumption that the interfacial bubble velocity is equal to a Stoke's law derived velocity:

$$v_g = a \langle R_g^{pore} \rangle^2 g \left(\frac{\rho_o - \rho_g}{18\mu_o} \right) \quad (3)$$

where $\langle R_g^{pore} \rangle$ corresponds to the average radius of a given gas structure, a is a constant that depends upon the pore-space connectivity, $\Delta\rho$ the density difference between oil and gas, g the gravitational constant. The velocity v_g used in this work was included in the range $[1.0-1.4] \times 10^{-5}$ m/s (just for comparison, in a much coarser sand with average throat pore radius of $77\mu\text{m}$, Corapcioglu's model predicts this velocity to be about $7 \cdot 10^{-3}$ m/s). Note that v_g is used microscopically as the filling velocity for a gas-oil interface moving upwards in a pore. To resume we can say that:

1. For a given gas cluster, this will become buoyant and move into an oil-filled pore i , of capillary entry radius r_i and at an height h_i above the bubble datum level (its base), if and only if:

$$Bo_{local}(h_i, r_i) = \frac{\Delta\rho g h_i}{2\sigma/r_i} > 1 \quad (4)$$

where we define Bo_{local} as the local Bond number (ratio gravity/capillarity).

2. Only 1 pore at a time (for a given gas structure) will be hosting a migrating gas/oil interface, the one for which Bo_{local} is highest, amongst all the computed Bo_{local} values.

An algorithm is currently under development to treat gravitational migration as a dynamic process in which multiple interfacial movements are considered. In fact it is probable that all the gas oil interfaces for which Eq. (4) is verified should be moving at the same time, and not only the one for which Bo_{local} is highest.

Method For Core Scale Simulations

Macroscale simulations were run on a 9.4 cm long network comprising 650X15X15 nodes, around half million pore elements, at laboratory rate (58 psi/day). In parallel, experimental data for depressurization in a 9.4 cm long dry Berea core, such as gas saturation history and in situ saturation profiles, were available for comparison with pore scale modeling. The network model is based on a regular lattice geometry with capillary elements that can be anchored to the experimental petrophysical sample (McDougall et al, 2001). The Berea core and network properties ($K=719\text{mD}$, $\phi=21\%$, $R_{\min}=1\mu\text{m}$, $R_{\max}=30\mu\text{m}$, pore length= $144\mu\text{m}$, co-ordination number= 6) are more extensively discussed in Piccavet et al (2006) as well as the PVT properties of the critical fluid C1/C10. Note that a constant diffusion coefficient was used ($D=2.0*10^{-5}\text{ m}^2/\text{day}$) whilst all other PVT data were treated as pressure dependent (gas-oil interfacial tensions, R_s , B_o , μ_g , μ_o , ρ_o , ρ_g).

DYNAMICS OF SOLUTION GAS DRIVE AT MACROSCALE

Bond Number Evolution vs Pressure

Figure 1 shows the evolution of the Bond number vs pressure. In particular for each bubble density situation Bo_{local} is plotted. At a given pressure P , a series of bubble migration events is taking place for any gas structure for which the condition $Bo_{local} > 1$ is locally satisfied. Therefore each plot corresponds to hundreds or even thousands of migration events at a given pressure P . The evolution of the Bond number for $Bo_{local} < 1$ is represented as a dashed line. The main points to be drawn from Figure 1 are the following:

- The maximum in Bo_{local} is higher and arrives earlier at lower bubble densities (1 bubble per 40,000 pores).
- At high bubble densities bubble migration is retarded until coalescence events make migration possible (1 bubble per 100 pores): in this case, a steep increase in Bo_{local} can be observed after coalescence.
- At a given pressure, a bubble break up event can take place which decreases the value h_i and therefore Bo_{local} : this has the potential to terminate bubble migration for one or more structures.
- The sharp maximum in Bo_{local} signifies that, at some point in the life of the gas structure/s and of the experiment/simulation, the physical length of the core simply “terminates”, and Bo_{local} cannot physically increase further.

These plots explain physically the history of gravitational effects in a solution gas drive experiment, the subtle balance with capillary forces and the non linearity brought in the process by coalescence events. Furthermore, since the peak in Bo_{local} (and the Bo_{local} function) is dependent on the core height, it could be speculated that recovery will be generally different for different core heights, at a constant bubble density per pore/oil volume.

Other Effects Of Bubble Density On The Process

Bubble Numbers Evolution

In light of the discussion presented above, the trends in bubble numbers as functions of pressure (Figure 2) become clear. At $P=P_{sat}=358.5$ bar different bubble densities are initially nucleated: the profiles stay constant or decrease as a result of coalescence. Eventually at a critical pressure, the condition $Bo_{local} > 1$ is satisfied and migration-imbibition events take place. In the formulation chosen here, snap-off events are always allowed; therefore migrating bubbles can break in several structures. This is the reason for the late increase in gas structure numbers: eventually capillarity dominates (increasing σ_{go}) and coalescence brings the numbers down again.

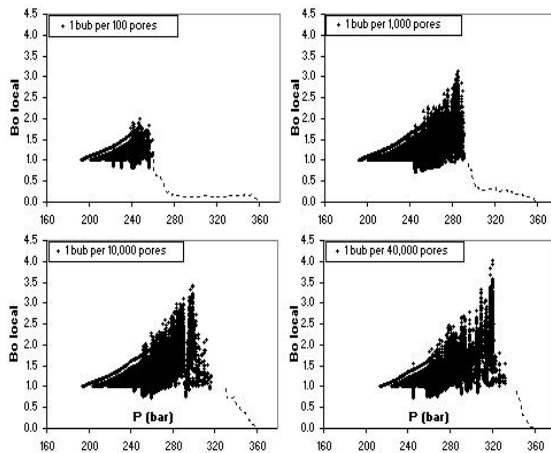


Figure 1. Evolution of the local Bond number versus pressure, for different bubble densities.

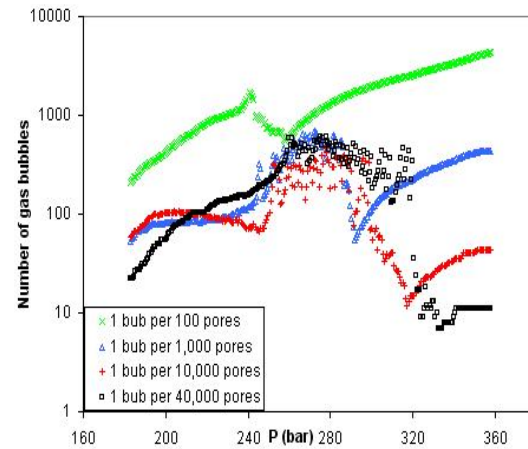


Figure 2. Evolution of bubble numbers vs pressure

Gas Saturation Evolution

Figure 3 shows the effects of different bubble density situations on gas saturation: as expected, the higher the bubble density, the higher the gas saturation and the recovery. For this system it appears that the correct bubble density to match the experiment would be somewhere between the cases 1 bubble per 10,000 pores and 1 bubble per 40,000 pores.

Gas Saturation Profiles

It is possible to compare the in situ measured experimental profiles with the simulated ones. This is shown in Figure 4 for three different bubble densities at a given pressure $P=270.7$ bar. It is seen that if the bubble density is very high (1 bubble per 100 pores) no gas cap forms: this is due to the fact that gravitational forces are lower (Bo_{local} peaks only to the value 2). For the lower number of bubbles (1 bubble per 40,000 pores) Bo_{local} peaks to 4 and a gas cap forms. It is noted that, although it is not possible to represent the core outlet boundary effects with the conditions adopted here, the lowest bubble density case represents experimental saturation data very well at this pressure below bubble point. The issue of gas saturation profiles (and more specifically their evolution versus pressure) is discussed in more detail below (see Figures 11, 13).

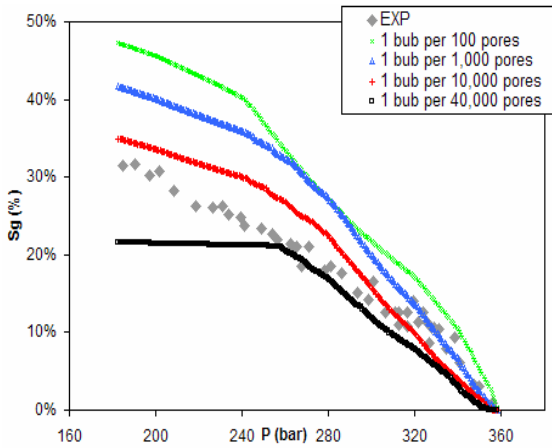


Figure 3. Evolution of gas saturation vs pressure

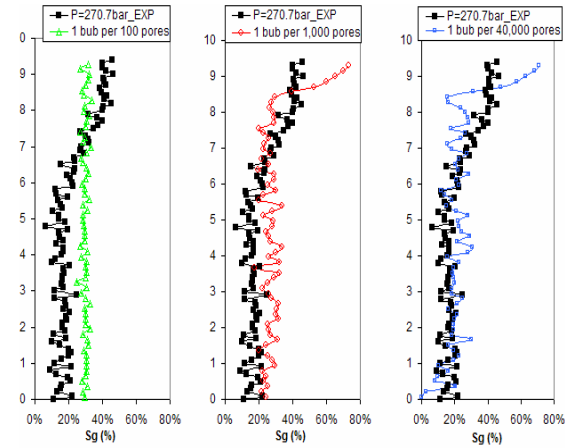


Figure 4. Evolution of saturation profiles for three different bubble densities

Gas Relative Permeabilities From Buoyancy

Since gas is flowing due to buoyancy, it could be possible to translate this flow into a gas relative permeability formulation. It is noticed that such flow is non Darcian. Here we propose to compute gas relative permeabilities for such a disconnected gas flow by adapting Darcy's law to the problem under examination. If the flow Q_g (which is measured during the simulation as gas volume exiting the network over a unit of time) is known and it is caused by a gravitational pressure gradient $\Delta\rho gh$, then the effective relative permeability of gas becomes:

$$K_g^{eff} = \frac{\mu_g Q_g}{A \Delta\rho g} \quad (5)$$

Here Q_g represents the flow of the disconnected gas phase only (which can be differentiated in the pore scale approach by the immobile or free gas phase), μ_g the gas viscosity, A the cross sectional area, $\Delta\rho$ the density difference between oil and gas and g the gravitational constant. It can be seen that K_g^{eff} does not depend on bubble height h (we assume the bubble is moving across its own network of gas filled pores of height h under a pressure gradient $\Delta\rho gh$). A similar approach was used by Javadpour and Pooladi-Darvish (2004) for the prediction of apparent gas relative permeabilities in viscous driven flow.

The gas relative permeability curves obtained with this formulation are shown in Figure 5 for the different bubble densities examined. It can be seen that:

- The curves are not monotonically increasing: buoyant gas flow does not occur throughout the depletion.
- For each bubble density there is a maximum in Krg (in most cases this stays constant for a while) which is achieved as a consequence of the limit in the number of migration events that are allowed in a given pressure step, consequence of Eq. (3). The onset of each of these curves indicates a critical gas saturation value Sgc : Sgc increases with bubble density (from 5% to 33%). This is defined as the gas saturation at which the first (disconnected) gas mobilization takes place.

Steady State Gas Relative Permeabilities

Figure 6 shows the gas steady-state relative permeabilities. These are calculated in a microscopic sub-network of dimensions 15X15X15 nodes positioned at the centre of the macroscale network (outside the reach of outlet boundary effects). A realistic assumption is made that K_{rg}/K_{ro} are non zero if the following two conditions are met simultaneously:

- a set of gas/oil filled pores continuously spans the microscale network of dimensions 15X15X15.
- the spanning clusters must be macroscopically connected (and therefore non trapped), to the outlet of the *macroscale* network (of dimensions 650X15X15).

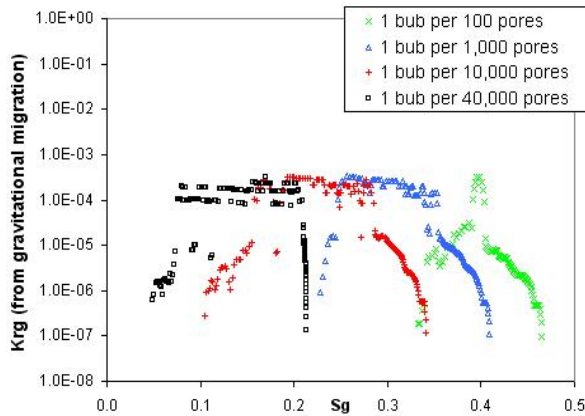


Figure 5. Gas relative permeability from buoyancy (unsteady state formulation)

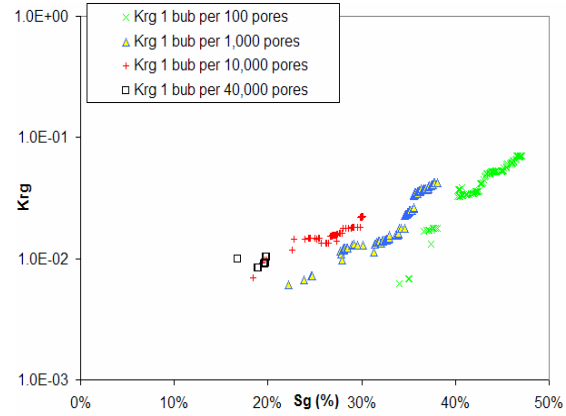


Figure 6. Steady state gas relative permeabilites

Note that gravitational effects act by perturbing the topology of the sample spanning gas cluster (whenever this has formed): therefore K_{rg} could become zero virtually at any stage during the simulation history if the gas cluster breaks microscopically (in the small central network) or macroscopically (on the way from the microscopic network to the top outlet). In Figure 6 this has happened for the lower bubble density (more prone to gravitational perturbation). In general once again, higher bubble densities produce higher critical gas saturations. Note that the steady state S_{gc} , symbolizing continuous gas flow is always higher than that corresponding to buoyancy-driven migration.

Height For Bubble Migration

Figures 7-8 show the height of migrating bubbles vs pressure for two different initial bubble densities. It can be concluded that:

- The bubble has to reach a critical size for it to become buoyant which is outside the reach of “conventionally sized” pore scale models: the minimum critical height is approximately 2 cm (1 bubble per 40,000 pores).
- The critical height for a bubble to become buoyant increases with bubble density: this is a consequence of the fact that at low bubble densities, growth takes place quickly and therefore the critical size for buoyancy is reached at a higher pressure, when gas-oil interfacial tension is lower.

- The maximum height of a bubble corresponds to the length of the core in these examples: at some point, there is a unique structure spanning the core.
- The bubble continues to migrate even when it spans the full network, as migration is taking place at the top open outlet (in other words the bubble is continuously migrating outwards).
- Break-up is especially evident for the lower bubble density case.

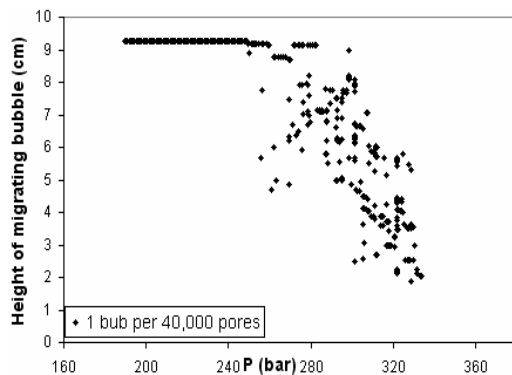


Figure 7. Height of migrating bubbles for the lower bubble density

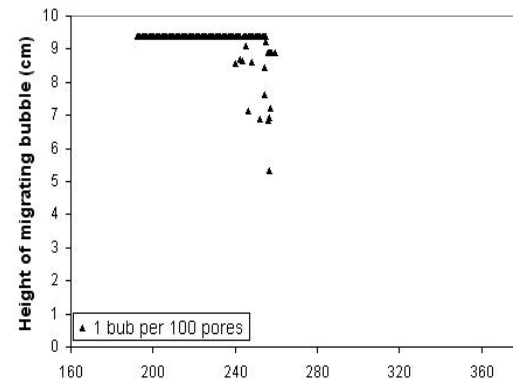


Figure 8. Height of migrating bubbles for the higher bubble density

Effects Of Scale

Sensitivities to different scales (core lengths) were performed (Figure 9 and 10). In Figure 9, for ease of comparison between the three cases, we plot the expected maximum in Bo_{local} at a given pressure, as from simulation data. It can be seen that the maximum possible gravity/capillarity ratio increases with the sample size, as expected. It could be speculated that core experiments performed at different scales will show a different force balance and therefore different production histories. Figure 10 shows that a longer core can become more gas saturated for the same bubble density: this behavior is difficult to explain at present but unpublished experimental data seem to confirm this observation. This issue could also be function of the adopted boundary conditions and will be investigated in future work.

Note that, so far, specific boundary conditions (named BC2, see discussion below) were used. The effect of boundary conditions was found to be relevant on both saturation histories and saturation gradients.

EFFECT OF BOUNDARY CONDITIONS AND GAS SATURATION PROFILES

The outlet boundary at the top of the core is usually simulated as a zero capillary pressure region. The limitations of this approach were discussed in Goodfield and Goodyear (2003) where an alternative outlet boundary interpretation for simulation was also proposed. It was noted by these authors that gas accumulation towards the top is a combined consequence of higher flow rates and the experimental set up at the outlet (grooved end cap, which would block some of the pore throats from conducting gas). If

the gas flow rate is high and some of the outlet pores are blocked, gas tends to accumulate and forms a gas cap.

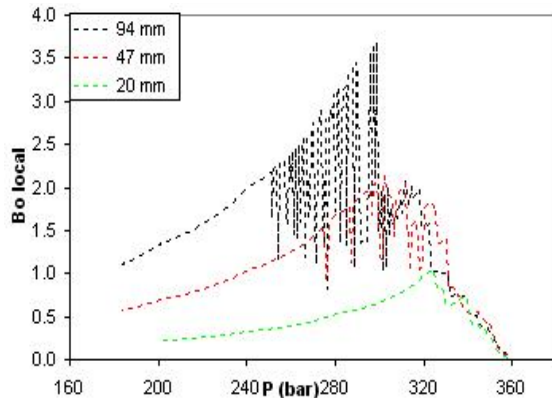


Figure 9. Effect of scale (core length) on the Bond number at a given bubble density

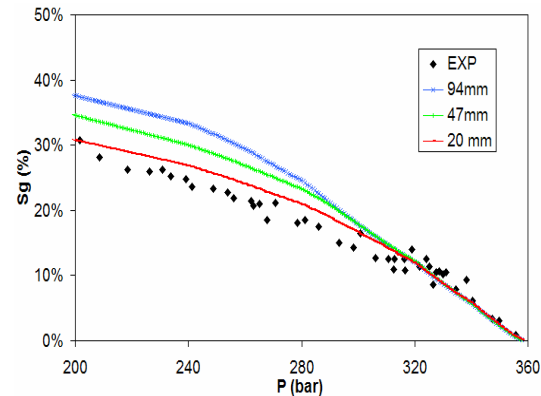


Figure 10. Effect of scale on gas saturation

To simulate the core conditions with a pore scale model, we can assume that the outlet pores are the ones from which gas leaves the system, in other words the outlet pores act as a production region. Therefore we could in theory simulate 4 different boundary conditions as:

- BC1. The outlet pores are plugged and gas cannot leave the model. This is equivalent to a closed network model where gas saturation eventually reaches $S_g=100\%$ if oil can always be displaced or $S_g=1-S_{or}$ if oil can remain trapped.
- BC2. The top outlet of the network model is open to gas only during the gas expansion (= withdrawal) phase: this condition was used so far in the paper and it could be speculated that this is the most relevant as gas can flow out of the core only at a given fixed (withdrawal) velocity dictated by the withdrawal rate (note that gravitationally driven bubble migration velocities are generally much higher than withdrawal velocities, therefore this high velocity gas would progressively accumulate at the top outlet).
- BC3. The top outlet of the network model is open to gas only during the gas migration phase: this simulates a situation where the gas that is produced out of the core is only the buoyant one.
- BC4. The top outlet of the network model is open to gas both during the gas expansion (= withdrawal) phase and the gas migration phase. This is equivalent to considering the network model as a part of a much larger sample: there are no boundary effects of gas retention. This condition could be used to compute relative permeabilities and capillary pressures directly for reservoir scenarios.

First a number of sensitivities are performed to investigate the issues discussed above relating to the grooved end cap blocking some of the outlet pores. For this purpose condition BC4 (no outlet pores plugged) is assumed and a fraction of the outlet pores is plugged (during both expansion and migration phases), according to size, until condition BC1 is reached. The result is shown in Figure 11 for a given bubble density: a very large

fraction of the outlet pores needs to be plugged for a gas cap to emerge (all pores with $r > 12.60 \mu\text{m}$). This could point to the fact that the grooved end cap might not be responsible for gas cap formation alone, unless this has a very low permeability.

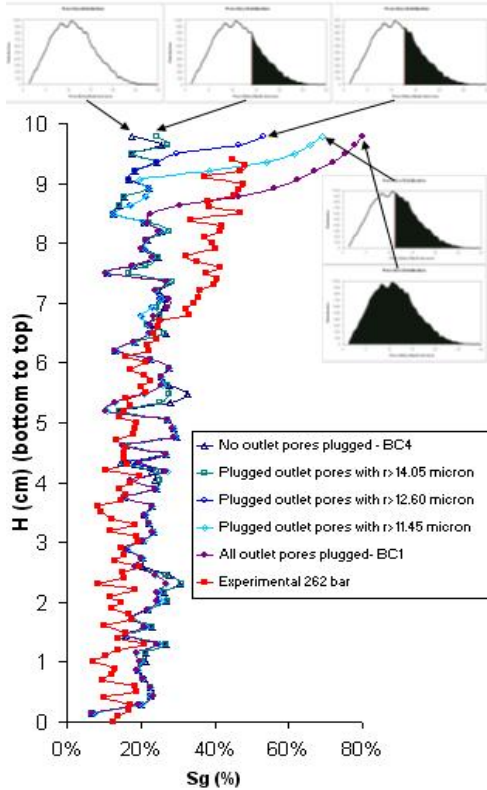


Figure 11. Simulated vs exp gas saturation profiles at $P=262$ bars. The fraction (in black) of the outlet pore size distribution that was plugged is also shown.

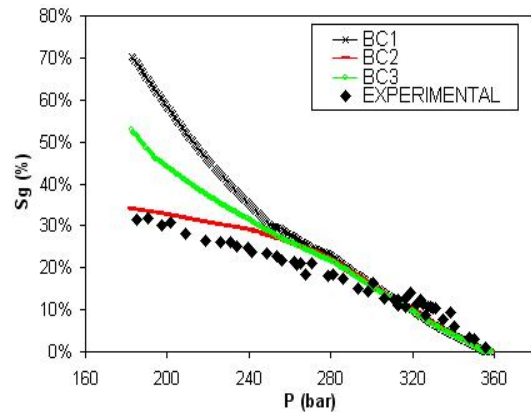


Figure 12. Gas saturation vs pressure for the experiment and two different realizations of the boundary conditions BC1, BC2 and BC3.

In Figure 12 we compare, for an optimal bubble density, gas saturations histories using boundary conditions BC1, BC2 and BC3 with experimental data. It can be seen that below $P=265$ bar the three curves diverge: the gas is now mostly produced outside the network model in BC2 and BC3. Since the shape of the simulated BC2 curve resembles quite closely the experimental one, we assume condition BC2 to be a good approximation to reality, at least for saturation histories. Figure 13 compares the gas saturation *profiles* for cases BC1, BC2, BC3 and experimental. We note that BC1 and, to a lesser extent BC3, reproduce the first gas cap formation at the same pressure as the experiment ($P=300.7$ bar). Furthermore, as the pressure is lowered, BC1 and BC3 show similar features in the propagation of the gas cap towards the bottom. On the other hand, although the qualitative agreement is good, these two boundary set-ups cause the network to be overall much more saturated than the core. With BC2, the gas cap appears at a lower pressure than the experiment and the front does not propagate downwards; nevertheless the network holds approximately the right gas saturation at any given pressure. Hence, the choice of boundary condition can effect both the overall saturation

in the core or the gas saturation profile: it is not possible to reproduce both using the same boundary condition at present.

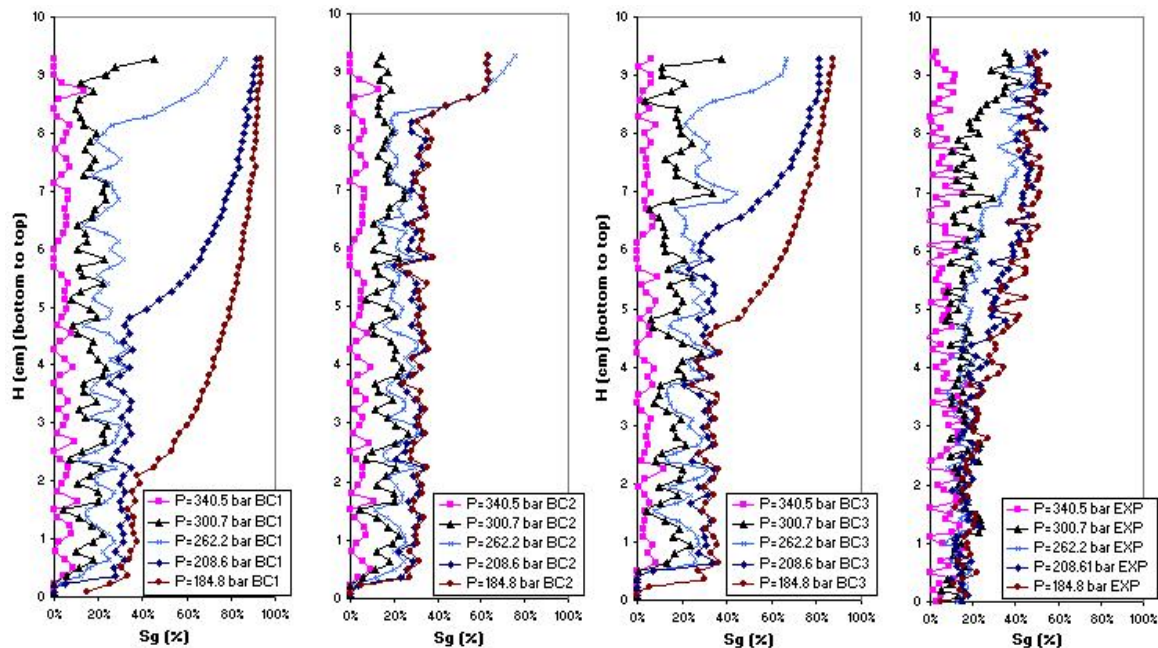


Figure 13. Simulated gas saturation profiles and experimental (right)

CONCLUSION

We have proposed a new formulation for pore network modeling where networks of laboratory size are simulated in a variety of scenarios. It is demonstrated that, using this approach, the core scale gravity to capillarity force balance can be reproduced without the need of any pore-to-core upscaling method. From this work we conclude that:

- Conventional pore scale simulation (using networks of limited dimension) cannot account for the experimental phenomenon of gravitational gas migration; only macroscale networks, such as those described here, should be considered.
- The evolution of the Bond number vs pressure is quite complex and depends on the physical height of the core/network, the bubble density and the degree of coalescence and bubble break-up.
- The core/network size is likely to have an effect on production performance since, for a given system height, the maximum gravity to capillarity force balance differs. Preliminary sensitivities show that, for this particular rock-fluid system and boundary conditions, gas saturation (and therefore oil production) increases with system height.
- The impact of buoyancy means that an alternative gas relative permeability formulation is required, as gas does not need to be connected to flow. As bubble densities increase (higher depletion rates) the buoyancy effect is delayed and will take place at higher saturations (with higher S_{gc}).
- A gas cap emerges in the simulation as a consequence of gravity. However, we have found that the upper outlet laboratory boundary condition cannot be easily simulated

at present and therefore the shape of the gas saturation profile is not well represented with declining pressure. It is hoped that the implementation of a new multi-pore gravitational migration algorithm will improve this situation.

ACKNOWLEDGEMENTS

The authors would like to thank Total for financial and technical assistance throughout the course of this study.

REFERENCES

1. Ayyalasomayajula, P., Kamath, J., Dehgani, K. and Fischer, D.: "Predicting primary depletion recovery of a giant light oil carbonate reservoir", presented at the SCA 2006 Symposium, Trondheim, paper SCA2006-17, 2006.
2. Bauguet, F., Egermann, P. and Lenormand, R.: "A new model to obtain representative field relative permeability for reservoirs under solution gas drive", SPE 84543, 2003.
3. Beecroft, W.J., Wood, A.R.O. and Rusinek, I.: "Evaluation of depressurisation, Miller Field, North Sea", SPE 56692, 1999.
4. Corapcioglu, M.Y., Cihan, A. and Drazenovic, M.: "Rise velocity of an air bubble in porous media: theoretical studies", Water Resour. Res., 40, W04214, 2004.
5. Drummond, A., Fishlock, T., Naylor, P. and Rothkopf, B.: "An evaluation of post-waterflood depressurization of the South Brae Field, North Sea", SPE 71487, 2001.
6. Egermann, P. and Vizika, O.: "Critical gas saturation and relative permeability during depressurization in the far field and the near-wellbore region", SPE 63149, 2000.
7. Goodfield, M. and Goodyear, S.G.: "Relative permeabilities for post-waterflood depressurization", SPE 83958, 2003.
8. Javadpour, F. and Pooladi-Darvish, M.: "Network modelling of apparent-relative permeability of gas in heavy oils", Journal of Canadian Petroleum Technology, vol. 43 (4), pp. 23-30, April 2004.
9. Kennedy, H.T. and Olson, R.: "Bubble formation in supersaturated hydrocarbon mixtures", Petroleum Transactions, AIME, vol. 195, pp. 271-278, 1952.
10. Ligthelm, D.J., Reijnen, G.C.A.M., Wit, K., Weisenborn, A.J. and Scherpenisse, D.J.: "Critical gas saturation during depressurization and its importance in the Brent Field", SPE 28475, 1997.
11. McDougall, S.R. and Mackay, E.J.: "The impact of pressure-dependent interfacial tension and buoyancy forces upon pressure depletion in virgin hydrocarbon reservoirs", Transactions IChemE, vol. 76, part A, pp. 553-561, 1998.
12. McDougall, S.R., Cruickshank, J. and Sorbie K.S.: "Anchoring methodologies for pore-scale network models: application to relative permeability and capillary pressure prediction", presented at the SCA 2001 Symposium, Edinburgh, Scotland, U.K., paper SCA2001-15, 2001.
13. Petersen, Jr, E.B., Agaev, G.S., Palatnik, B., Ringen, J.K., Øren, P.E. and Vatne, K.O.: "Determination of critical gas saturation and relative permeabilities relevant to the depressurization of the Statfjord Field", presented at the SCA 2004 Symposium, Abu Dhabi, paper SCA2004-33, 2004.
14. Piccavet, N., Long, J., Hamon, G., Bondino, I. And McDougall, S.R.: "Depletion of near-critical oils: comparison between pore network model predictions and experimental results", proceedings, presented at the SCA 2006 Symposium, Trondheim, paper SCA2006-32, 2006.
15. Skauge, A., Haskjold, G. Ormehaug, P.A. and Morten Aarra, M.: "Studies of Production under bubblepoint", proceedings, presented at IOR/EAGE Symposium, paper 2076, Brighton, U.K., August 1999.